Symmetry Laws for Interaction between Helical Macromolecules

A. A. Kornyshev* and S. Leikin#

*Research Center "Jülich," D-52425 Jülich, Germany; and #Laboratory of Physical and Structural Biology, National Institute of Child Health and Human Development, National Institutes of Health, Bethesda, Maryland 20892 USA

ABSTRACT The power of symmetry laws is applied in many scientific areas from elementary particle physics to structural biology. The structures of many biological helices, including DNA, were resolved with the use of pertinent symmetry constraints. It was not recognized, however, that similar constraints determine cardinal features of helix-helix interactions vital for many recognition and assembly reactions in living cells. We now formulate such symmetry-determined interaction laws and apply them to explain DNA "over-winding" from 10.5 base pairs per turn in solution to 10 in hydrated fibers, counterion specificity in DNA condensation, and forces observed over the last 15 Å of separation between DNA, collagen, and four-stranded guanosine helices.

INTRODUCTION

Surfaces of most biological helices bear charged residues and adsorbed ions. These charges form complicated patterns, often preserving elements of underlying helical symmetry. The electrostatic potential near a helical molecule reflects this structure and may affect the choice between various molecular conformations, as shown for DNA in dilute solution (Bailey, 1973; Jayaram and Beveridge, 1990; Jayaram et al., 1989; Soumpasis, 1978; Wagner et al., 1997). The charge pattern symmetry may have even more dramatic effect on intermolecular interactions. Indeed, model osmotic stress experiments in columnar phases of DNA (Rau et al., 1984), collagen (Leikin et al., 1994), guanosine helices (Mariani et al., 1998; Mariani and Saturni, 1996), and several polysaccharides (Rau and Parsegian, 1990) revealed unexpected forces which could not be interpreted as the interaction between charged rods. It was not clear whether this was due to the non-electrostatic nature of the forces or to failure to take into account the symmetry of helical charge patterns. To resolve this issue we developed mathematical background of a theory of helix-helix forces that accounts for discrete patterns of solvated surface groups (Kornyshev and Leikin, 1997). Here we use it to formulate general relationships between symmetry and force and show the latter in action.

THEORY

Linearized Poisson-Boltzmann model

An analytical solution (Kornyshev and Leikin, 1997) for the energy of interaction between two molecules with parallel cylindrical, water-impermeable inner cores and arbitrary patterns of surface charges has a form of a sum of "interaction modes,"

$$E_{\mathrm{int}}(R) = \frac{1}{2}\sum_{\mathrm{q}=-\infty}^{\infty}\sum_{\mathrm{n,m}=-\infty}^{\infty}\sum_{\nu,\mu=1}^{2} Q_{\mathrm{n,m}}^{\nu,\mu}(q,R)\,s_{\mathrm{n,m}}^{\nu,\mu}(q). \quad (1)$$

The contribution of each mode is a product of the surface charge density structure factor,

$$s_{\mathrm{n,m}}^{\nu,\mu}(q) = \int_0^{2\pi}\frac{d\phi}{2\pi}\,e^{\mathrm{in}\phi}\int_0^{2\pi}\frac{d\phi'}{2\pi}\,e^{-\mathrm{im}\phi'}\int_{-\mathrm{L}/2}^{\mathrm{L}/2}dz\,e^{\mathrm{i}qz}\int_{-\mathrm{L}/2}^{\mathrm{L}/2}\frac{dz'}{L}$$
$$\left\{\frac{\sigma_\nu(z+z',\phi)\sigma_\mu(z',\phi') + \sigma_\mu(z+z',\phi)\sigma_\nu(z',\phi')}{2}\right\}, \quad (2)$$

and the field "propagator," $Q_{\mathrm{n,m}}^{\nu,\mu}(q, R)$. Here R is the interaxial distance; L is the length of the helices; ν, $\mu(=1, 2)$, label the molecules; the integers n and m number angular Fourier harmonics of the surface charge density σ_ν in cylindrical coordinates (z, ϕ) associated with the molecular axis; the argument $q = 2\pi k/L$ numbers the axial harmonics (k is an integer). The exact expressions for $Q_{\mathrm{n,m}}^{\nu,\mu}(q, R)$ are cumbersome (Kornyshev and Leikin, 1997). The following, simplified ones (valid when $\tilde{q}(R - a_1 - a_2) \geq 1$ and the surface charges lie directly at the core/water interface) are sufficiently accurate for most applications.

$$Q_{\mathrm{n,m}}^{\alpha,\beta}(q,R) \approx (-1)^{\beta\mathrm{n}-\alpha\mathrm{m}}\frac{8\pi^2}{\epsilon\tilde{q}^2}\frac{K_{\mathrm{n-m}}(\tilde{q}R)}{K'_{\mathrm{n}}(\tilde{q}a_\alpha)K'_{\mathrm{m}}(\tilde{q}a_\beta)} \propto \exp(-\tilde{q}R) \quad (3)$$

$$Q_{\mathrm{n,m}}^{\alpha,\alpha}(q,R) \approx -(-1)^{\beta(\mathrm{n}-\mathrm{m})}\frac{8\pi^2}{\epsilon\tilde{q}^2}\sum_{\mathrm{j}=-\infty}^{\infty}$$
$$\left[\frac{K_{\mathrm{n-j}}(\tilde{q}R)K_{\mathrm{j-m}}(\tilde{q}R)I'_{\mathrm{j}}(\tilde{q}a_\beta)}{K'_{\mathrm{n}}(\tilde{q}a_\alpha)K'_{\mathrm{m}}(\tilde{q}a_\alpha)K'_{\mathrm{j}}(\tilde{q}a_\beta)}\right] \propto \exp(-2\tilde{q}R) \quad (4)$$

Here $\alpha, \beta = 1, 2$, $\alpha \neq \beta$, $\tilde{q} = \sqrt{q^2 + \lambda_0^{-2}}$, λ_0 is the Debye length, a_ν is the molecular radius, ϵ is the water dielectric

Received for publication 1 June 1998 and in final form 7 August 1998.

Address reprint requests to Dr. Sergey Leikin, Laboratory of Physical and Structural Biology, NICHD, NIH, Bldg. 12A, Rm. 2041, Bethesda, MD 20892. Tel: 1-301-496-1121; Fax: 1-301-496-2172; E-mail: leikin@helix.nih.gov.

© 1998 by the Biophysical Society

0006-3495/98/11/2513/07 $2.00

constant, K_n and I_n are the modified Bessel functions of nth order, $K_n'(x) = dK_n(x)/dx$, $I_n'(x) = dI_n(x)/dx$. The propagators decrease exponentially with the characteristic lengths.

$$\lambda^{\alpha,\beta}(q) = 1/\tilde{q} = 1/\sqrt{q^2 + 1/\lambda_0^2} \text{ and } \lambda^{\alpha,\alpha}(q) = 1/2\tilde{q}. \tag{5}$$

Modes with smaller q have larger decay lengths. Note that $Q_{n,m}^{\alpha,\beta}(q, R)$ increases with $|n - m|$. Therefore, the modes with $m = -n$ (dominant in the interaction of molecules of opposite handedness) are stronger than the modes with $m = n$ (dominant in the interaction of molecules of the same handedness).

The $q = n = m = 0$ mode describes interaction between homogeneously charged cylinders. It dominates for highly charged helices, but it becomes negligible, compared to the other modes, with increasing fraction of adsorbed counterions. The $\nu \neq \mu$, $q \neq 0$ modes represent direct interactions between charges on opposing helices. At a favorable mutual alignment of the molecules (achieved, e.g., by rotation around the long axis), the sum of these modes gives an attraction which may cause spontaneous aggregation. The $\nu = \mu$, $q \neq 0$ modes represent repulsive image-charge forces (hence their decay lengths are two times shorter than for modes with the same q but $\nu \neq \mu$). These modes hamper the molecular contact.

Note that the linearized Poisson-Boltzmann model may be inaccurate near highly charged surfaces. However, at distances larger than a characteristic length of nonlinear electrostatic screening by ionic atmosphere, the linearized solution is a reasonable approximation. Specifically, Eqs. 1 and 2 describe the leading quadratic terms of the net force expansion with respect to Fourier harmonics of the surface charge density; Eqs. 3–5 can be used for the distance dependence of the interaction modes, although the preexponential factors may be different because of nonlinear effects.

At surface-to-surface separations close to the nonlinear screening length, Eqs. 1 and 2 may not work. However, at very small distances between helical surfaces, e.g., in dense aggregates where helices are in direct contact and only a few water molecules remain in DNA grooves, these equations may become a good approximation again. These water molecules are likely to exhibit only limited motion. Assuming that their dielectric screening ability is low, one can treat the aggregate as a continuous, homogeneous dielectric medium with a low dielectric constant. By describing all counterions explicitly as discrete charges and solving Poisson equation for the electric field one again arrives at Eqs. 1 and 2 although with different interaction propagators $Q_{n,m}^{\nu,\mu}$. This solution and analysis of its main features are reported elsewhere (Kornyshev and Leikin, 1998).

Mode selection rules

Invariance of surface charge density with respect to specific symmetry transformations results in selection rules defining which interaction modes may have nonzero amplitude. For example, charge density on a right-handed helix with equidistant residues is invariant with respect to an axial shift upward by kh with a counterclockwise rotation by $2\pi kh/H$,

$$\sigma_\nu\left(z + kh, \phi + 2\pi k\frac{h}{H}\right) = \sigma_\nu(z, \phi) \tag{6}$$

where h is the axial rise per charged residue, H is the helical pitch, and k is an integer. When the two helices are identical, we find from Eqs. 1, 2, and 6 that only the modes with

$$m - n = J\frac{H}{h}, \quad q = j\frac{2\pi}{h} - n\frac{2\pi}{H} \qquad (j, J = 0, \pm 1, \pm 2, \ldots, \pm\infty) \tag{7}$$

have nonzero amplitudes. Selection rules for several other helical structures are given in Table 1.

These selection rules are based exclusively on the symmetry of the surface charge density. They are valid as long as Eqs. 1 and 2 are applicable, regardless of the specific form of interaction propagators; i.e., the same selection rules apply when distances between helical surfaces are larger than a characteristic length of nonlinear electrostatic screening and when helices are in direct contact in a dense aggregate. Specifically, an estimated value of the nonlinear screening length for DNA is ~1–3 Å, depending on the assumptions with respect to surface charge density and dielectric properties of water in the first solvation shell. There is no good analytical theory for such surface separations. Still, one might expect the selection rules to remain reasonably accurate even then, because these rules apply on both ends of this rather narrow distance range.

Energies of interaction between *B*-DNA molecules

We calculated the interaction energies plotted in Figs. 1 and 2 from Eqs. 1–4 by assuming a regular pattern of point-like phosphate charges. The medium response parameters (ϵ and λ_0) were estimated from measured (Rau et al., 1984; Rau and Parsegian, 1992b) force-distance curves for hydrated Na-DNA fibers. It is important to keep in mind that effective values of water dielectric constant and Debye length inside DNA fibers may be significantly different from those in bulk electrolyte solution and that hydration forces may contribute to the interaction energy as well.

Energetic cost of water restructuring around solvated residues was proposed to be responsible for forces which can be equally or even more important than the electrostatic ones. This idea of hydration forces is still being debated (Israelachvili and Wennerstrom, 1996; Leikin et al., 1993; McIntosh and Simon, 1994; Parsegian and Evans, 1996). However, a wealth of supporting evidence has been collected for biological helices (Kuznetsova et al., 1997; Leikin et al., 1994, 1995, 1997; Mariani and Saturni, 1996; Rau et al., 1984; Rau and Parsegian, 1990, 1992a,b). The formal-

ism suggested here, including the selection rules, is directly applicable to a mean-field model of hydration forces based on similar equations (Kornyshev and Leikin, 1989). In this model solvated surface residues, charged or not, play the role of sources of hydration field; an empirical constant replaces ϵ^{-1} and λ_0 ($\approx$4 Å) stands for a correlation length in water (Kornyshev and Leikin, 1997).

The elastic energy of DNA overwinding from 10.5 to 10 bp/turn was estimated as $E_{\text{tors}} \approx 1.2\ 10^{-7}$ erg/cm using the torsional rigidity $C = 3\ 10^{-19}$ erg/cm (Crothers et al., 1992).

RESULTS AND DISCUSSION

Thus, an electrostatic force between two helices with parallel long axes may be described as a weighted sum of static interaction modes distinguished by two integer indices n and m and one real index q. Each mode represents a force between two rods with static surface charge densities that vary as $\sin(n\phi_1)$ and $\sin(m\phi_2)$ with the angles ϕ_1 and ϕ_2 around the axes of the first and the second rod, respectively, and depend on the axial coordinate z as $\sin(qz)$. These modes are repulsive or attractive and have different amplitudes and distance dependencies. A change in the balance between them affects the net force dramatically. The charge pattern symmetry imposes constraints on the "wave numbers" n, m, and q in the form of relationships between them, i.e., selection rules (see Theory). These relationships define the allowed modes which give nonzero contribution to the force. All other modes are forbidden. For homogeneously charged rods, $n = m = q = 0$. Helical symmetries establish more complicated relationships, examples of which are drawn in Table 1. To illustrate how these selection rules work, consider the following examples.

DNA overwinding in fibers

The structure of the DNA double helix has been solved (Watson and Crick, 1953; Wilkins et al., 1953), but some aspects of this structure remain puzzling to this day (Saenger, 1984). For instance, B-DNA molecules have $\sim$10.5 basepairs (bp) per turn in solution and 10 bp/turn in columnar fibers (Saenger, 1984). In dehydrated fibers at low relative humidity, this could be explained by steric requirements of direct intermolecular contacts. However, the number of basepairs per turn does not change when the fibers are wetted so that neighboring DNA molecules are separated by up to 10–15 Å of water (Rhodes and Klug, 1980; Zimmerman and Pheiffer, 1979). It was pointed out that this must be caused by some intermolecular interaction through the water layer (Rhodes and Klug, 1980).

The symmetry rule S.4 (Table 1) rationalizes a likely origin of this phenomenon. It says that the number of allowed interaction modes is different when DNA helices have integral versus nonintegral numbers of bp/turn. Some energetically favorable modes allowed at integral bp/turn are forbidden at nonintegral bp/turn. These modes are associated with alignment of phosphates on DNA surface into 10 charged ridges parallel to the main axis and separated by longitudinal grooves (Fig. 1). An alignment with the charged ridge on one molecule facing a groove on the other one minimizes unfavorable interactions of phosphates. The plot in Fig. 1 shows an estimate for the corresponding energy gain. It suggests that the energetic advantage of 10 bp/turn relative to $10 + x$ bp/turn ($0 < x < 1$) may exceed the cost of the required torsional deformation. The interaction gives DNA an incentive to overwind to 10.0 bp/turn upon aggregation into fibers.

Counter-ion-induced DNA condensation

Condensation of DNA from an aqueous solution into an ordered columnar aggregate of hydrated helices is induced by a number of polyvalent and some divalent cations (Bloomfield, 1996; Knoll et al., 1988; Pelta et al., 1996; Rau and Parsegian, 1992a,b; Widom and Baldwin, 1983). For example, Mn^{2+} and Cd^{2+} condense DNA (Knoll et al.,

TABLE 1 Selection rules for modes of interaction between two helices with parallel axes

	Helical symmetry	Allowed modes*
S.1	Two helices of the same handedness, right (−) or left (+), with homogeneously charged strands	$m = n,\ q = \mp\ n\frac{2\pi}{H}$
S.2	One right- and one left-handed helix with the same pitch and homogeneously charged strands[#]	$m = -n,\ q = n\frac{2\pi}{H}$
S.3	Right- or left-handed helices with N_s equally-spaced strands	$n = kN_s,\ m = KN_s,\ k, K = 0, \pm1, \pm2, \ldots \pm\infty$
S.4	Right- (−) or left- (+) handed helices with a regular axial rise h per charged residue on each strand	$m - n = J\frac{H}{h},\ q = j\frac{2\pi}{h} \mp n\frac{2\pi}{H},\ j, J = 0, \pm1, \pm2, \ldots \pm\infty$
S.5	Right- (−) or left- (+) handed helices with positive and negative charges on net-neutral strands	$q \neq \mp\ n\frac{2\pi}{H},\ q \neq \mp\ m\frac{2\pi}{H}$

H is the helical pitch; H/h is the number of residues per helical turn.

*Only the modes that satisfy the right column constraints have nonzero amplitudes. Combination of selection rules is possible when several symmetry conditions apply simultaneously. For example, rules S.4 and S.5 may apply simultaneously to DNA if it is neutralized by counterions bound to phosphate strands.

[#]Most biological interactions occur between helices of the same handedness (all selection rules except S.2 are thus derived for this case). However, only helices of opposite handedness, which are mirror images of each other, may have fully complementary charge patterns. They would efficiently recognize each other via attractive $m = -n$ modes which are much stronger than the corresponding $m = n$ modes for helices of the same handedness. Therefore, common recognition and assembly reactions between helices of the same handedness utilize specific, partially complementary patterns.

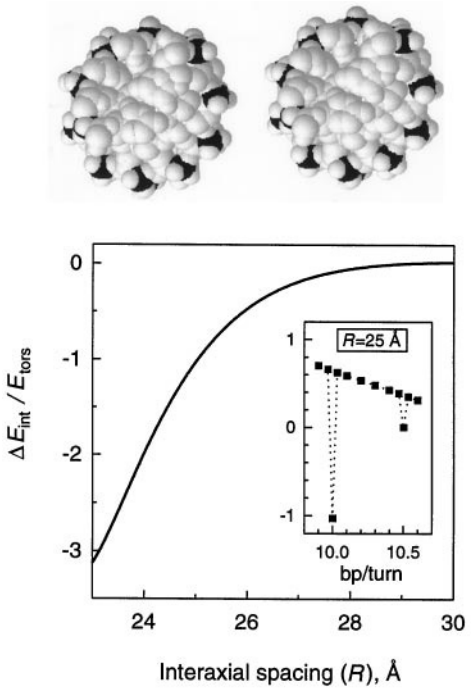

FIGURE 1 *Integer number of base pairs (bp) per turn promotes DNA-DNA recognition in water.* The top view on B-DNA dodecamers (Edwards et al., 1992) illustrates axial phosphate ridges which form at integer number of bp/turn (phosphate atoms are painted black). The ridge-to-groove alignment of opposing helices minimizes unfavorable phosphate-phosphate interactions upon overwinding of DNA from 10.5 to 10 bp/turn. The graph below gives an estimate (see Theory) of the corresponding gain in electrostatic interaction energy per molecule in wet columnar fibers, ΔE_{int}. This energy gain exceeds the cost of the torsional deformation, E_{tors}, favoring spontaneous overwinding at interaxial spacings $R \leq 25$ Å. Experiments (Rhodes and Klug, 1980; Zimmerman and Pheiffer, 1979) show that the overwinding occurs at $R \leq 30$–35 Å. This is not surprising since we did not account for a number of factors which may greatly enhance this effect, extending it to larger intermolecular distances. For example, more detailed calculation shows that counterion adsorption may increase the energy gain associated with DNA overwinding by up to an order of magnitude. The enhancement factor depends on the specific location of counterions, which is not exactly known.

The insert shows that the interaction energy (plotted at $R = 25$ Å) has deep minima at 10 and 10.5 bp/turn. In fact, axial alignment of phosphates leads to local minima at every rational (versus irrational) number of bp/turn, but the depths of other minima are negligibly small. This is described by the selection rule S.4, Table 1, which restricts the number of allowed modes responsible for the energetically favorable alignment. At 10 bp/turn ($H/h = 10$) the constraint $m - n = J(H/h)$ is satisfied for any running integer J. At 10.5 bp/turn ($H/h = 10.5$), it is fulfilled only for even J. All $J \neq 0$ are forbidden at irrational H/h.

Finite size of phosphate groups and weak disorder in their location practically eliminate the dips in the interaction energy at rational but nonintegral H/h, with only minor influence on the dips at integral H/h.

1988; Rau and Parsegian, 1992a,b), but Ca^{2+} or Mg^{2+} do not (Bloomfield, 1996; Rau and Parsegian, 1992a). A key to this specificity may lie in different symmetries of cation adsorption pattern, e.g., in-groove versus on-strand localization. The in-groove adsorption allows a complementary alignment with positively charged grooves on one helix facing negatively charged strands on the other (Fig. 2). This causes DNA-DNA attraction, via modes with $q = -2\pi n/H$, where H is the helical pitch. The attractive $q = -2\pi n/H$ modes are forbidden in the case of on-strand localization, as prescribed by rule S.5 of Table 1. The on-strand versus off-strand adsorption of cations, thus, reduces the attraction between DNA molecules (Fig. 2) and inhibits their aggregation. Therefore, cations with high affinity to phosphates (as Ca^{2+} or Mg^{2+}) may have weak or no condensing effect.

Note that the adsorption pattern symmetry may differ from the symmetry of the charged phosphate backbone, depending on the cation nature. This would allow new attractive modes which are otherwise forbidden by the backbone symmetry. Understanding the strong precipitating ability of $Co(NH_3)_6^{3+}$ and polyamines (Bloomfield, 1996; Gosule and Schellman, 1978; Pelta et al., 1996; Rau and Parsegian, 1992b; Widom and Baldwin, 1983) may, therefore, come with better knowledge of their adsorption pattern.

Exponential short-range forces

Repulsive forces, exponentially decaying with the separation, were measured at the last 10 Å between surfaces of guanosine helices (Mariani and Saturni, 1996), collagen (Leikin et al., 1994; Leikin et al., 1995), and DNA in the presence of condensing counterions (Rau and Parsegian, 1992a,b). Surprisingly, the force decay lengths were practically independent of the solution ionic strength and were much shorter than the Debye length (Table 2) in contrast to the theory of interaction between homogeneously charged rods.

This behavior can be explained as follows. Each of the helices has a large number of surface charges but the net charge is small, because of countercharges adsorbed or intrinsic to the molecule. The force determined by the average charge (the $q = n = m = 0$ mode) is, thus, suppressed. The electrostatic interaction at small separations is dominated by the image-charge repulsion of discrete surface charges from the low-dielectric-constant core of the opposing molecule. The corresponding $q \neq 0$ modes (see Theory) exponentially decay with the characteristic lengths $\lambda = 1/2\sqrt{q^2 + 1/\lambda_0^2}$ which depend on the Debye length (λ_0) and on the wave number q. The pertinent selection rules define the allowed values of q. The modes with the smallest allowed q dominate. The decay length, thus, depends on the charge pattern symmetry. When $\lambda_0 q \gg 1$, the decay length practically does not depend on the ionic strength, $\lambda \approx 1/2q$.

For guanosine helices, the dominant q is $\pm 2\pi N_s/H$, where $N_s = 4$ is the number of strands and $H = 40.8$ Å is the helical pitch (Table 2). This gives $\lambda \approx H/(4\pi N_s) \approx 0.7$ Å, salt-independent (up to ~1–2 M), in agreement with the experiment.

For DNA, the dominant modes are those with $q = \pm 2\pi/H$ and $q = \pm 4\pi/H$ (Table 2). The force is a weighted sum of two exponentials with the decay lengths determined mostly by the pitch $H = 34$ Å, but weakly dependent on the ionic strength. The calculated range of λ is in line with the measured one (Table 2).

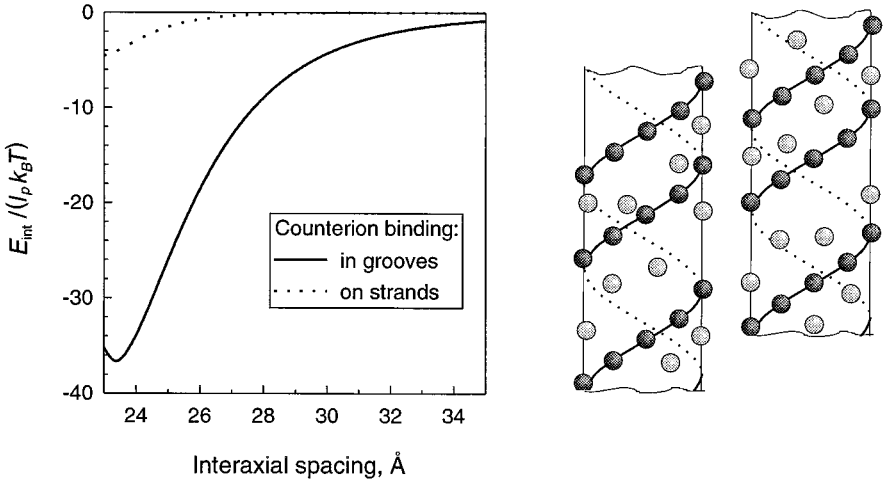

FIGURE 2 *Counterion binding pattern regulates DNA-DNA recognition.* Cation binding into grooves results in negatively charged strands and positively charged grooves and enables strand-to-groove charge complementarity between opposing molecules. A sketch on the right hand side illustrates a possible alignment of this type. In the sketch, phosphates and counterions are shown by dark and light spheres correspondingly. This favorable alignment promotes attraction between the helices. The graph on the left hand side shows the energy of interaction (E_{int}) between two identical B-DNA molecules in the units of thermal energy ($k_BT \approx 4\ 10^{-14}$ erg at 300°C) per persistent length ($l_p \approx 500$ Å), calculated from Eqs. 1–4. Counterion binding into grooves leads to stronger attraction (*solid line*) than binding onto the phosphate strands (*dotted line*).

Charge pattern on collagen surface is not regular, despite the helical symmetry of the protein backbone. Therefore, the expected electrostatic image force may have components with any q, it is not exponential, it should strongly depend on the ionic strength, and it should decay slower than the measured repulsion with 0.7 Å decay length (Table 2). The discrepancy with the observed behavior is too large to be explained by small uncertainties in model parameters, indicating that the measured force is not electrostatic. Experiments (Bella et al., 1994, 1995; Kuznetsova et al., 1997; Leikin et al., 1994, 1995, 1997) suggested that this is a hydration force associated with the energetic cost of hydrogen-bond network rearrangement in the separating water. If so, the same symmetry principles may apply. The collagen hydration pattern is determined mostly by the helical protein backbone symmetry (Bella et al., 1994, 1995; Fraser and MacRae, 1973) in contrast to the charge pattern. The decay length of the hydration force, prescribed by selection rule S.1, is determined by the helical pitch, $\lambda \approx H/4\pi \approx 0.7$ Å, in agreement with the experiment (Table 2).

Note that hydration may as well contribute to the forces between DNA (Rau et al., 1984; Rau and Parsegian, 1992a,b) and between guanosine helices (Mariani et al., 1998; Mariani and Saturni, 1996) where the hydration pattern is defined by charged phosphates, i.e., it has the same symmetry as the charge pattern. Therefore, electrostatic and hydration forces are expected to have similar features. The difference between their amplitudes depends on poorly known factors (water dielectric response between the macromolecules, nonlinear charge screening, energy of water

TABLE 2 Effect of helical symmetry on the short-range, exponential repulsive forces between biological helices

Structure			Theory				Experiment		
Molecules	H (Å)	N_s	Selection rules (from Table 1)	Dominant modes*	λ_{theor} (Å) (electrostatic)	λ_{theor} (Å) (hydration)	λ_{exp} (Å)	Debye length λ_0 (Å)	Reference
Condensed B-DNA	34	2	S.4	$q = \pm 2\pi/H, \pm 4\pi/H, m = n = \pm 1, \pm 2, j = J = 0$	1.2–2.6	1.1–1.6	1.3–1.5	6–20	Rau and Parsegian, 1992a,b
Guanosine helices	40.8	4	S.3 and S.4	$q = \pm 2\pi N_s/H, m = n = \pm N_s, k = K = \pm 1, j = J = 0$	0.65–0.75	0.7	0.7	2–30	Mariani and Saturni, 1996
Collagen	9.6	3	*Electrostatic*: S.5 *Hydration*: S.1	*Electrostatic:* $0 < \lvert q \rvert < 2\pi/H$ *Hydration*: $q = \pm 2\pi/H$	≥5	0.7	0.7	>20	Leikin et al., 1995

λ_{exp} are the measured decay lengths, $\lambda_{theor} = 1/2\sqrt{q^2 + 1/\lambda^2_0}$ are the decay lengths calculated for dominant modes. Electrostatic and hydration forces may differ in the set of dominant modes and in the value/meaning of λ_0 which is either the Debye length (determined by the ionic strength) or a structural correlation length (≈4 Å, in water), respectively.

*Only one mode dominates and the net force is a single exponential when the helices are single-stranded, multi-stranded but have tightly clustered strands and a single large groove (as collagen), or multi-stranded with equally spaced strands (as guanosine). Two or more modes dominate when double- or multi-stranded helices have several well-resolved grooves of different widths (Kornyshev and Leikin, 1997). Then, the net force is a weighted sum of several exponentials. In particular, the double-exponential decay in B-DNA results from the two modes with different q and a larger preexponential factor for the mode with the larger q.

hydrogen-bond rearrangement, etc.). The two force mechanisms are hard to distinguish, but the symmetry arguments can be applied regardless of the outcome of this ongoing quest.

Outlook

Thus, seemingly "nonphysical" short force decay lengths <1 Å, DNA overwinding in wet fibers, and counter-ion specificity of DNA condensation find a common rationale as symmetry-driven collective effects. This experimental evidence suggests that our model plausibly explains phenomena observed when helices are separated by several layers of water molecules, e.g., in wet DNA, guanosine, and collagen fibers. However, at this point other explanations cannot be excluded. The theory requires further development and experimental verification until its applicability to biological phenomena is proven.

The present study is only a first necessary step. Many phenomena still remain to be examined. For instance, we have presented a simplified static picture of helices with an idealized order in positions of surface charged groups. In reality, thermal motions of the groups can be neglected only when the energy of intermolecular interaction significantly exceeds corresponding thermal energy (1 k_BT per persistence length). This is, indeed, the case for the solid curve in Fig. 2. Thermal motions may become important when the interaction energy is comparable to 1 k_BT or lower. To some extent, we imply this in our analysis. (This is precisely the reason we presume that the attraction shown by the dotted curve in Fig. 2 is unlikely to cause DNA aggregation). In the latter case, one may also expect a change in the mode balance and some broadening of the peaks in the corresponding surface charge density structure factors. As a result, not only the modes with q, n, m defined by the selection rules but also modes with q, n, m in a vicinity of these values may become allowed, though with reduced amplitudes. Similar "smearing" of the selection rules may be induced by quenched disorder when "errors" in positions of the groups accumulate along helical strands. Some of these issues may become important in various specific cases, and we will address them separately. However, the agreement with the experiments suggests that the symmetry principles formulated here may prove to be a good starting point for understanding complex rules of interaction between biological helices.

We have focused here on pairwise interactions of highly hydrated helices. Most interactions in fibers are pairwise additive, but full optimization of all pairwise interactions is constrained by fiber packing symmetries, i.e. the symmetry of interactions may affect the packing and vice versa. This should be particularly important in dense aggregates of helical molecules containing little or no water which are also common in biological systems. The present theory does not apply under such conditions. The appropriate modification of the theory is, nonetheless, possible (Kornyshev and Leikin, 1998). One of the most challenging related issues we are currently working on is understanding the contribution of inter-helix interactions into the observed structural polymorphism of DNA.

We are grateful to V. I. Ivanov, V. A. Parsegian, D. C. Rau, P. Steinbach and V. B. Zhurkin for stimulating discussions. A. A. K. thanks the National Institutes of Health for financial support of his visits to Bethesda.

REFERENCES

Bailey, J. M. 1973. The electrostatic potential of a discretely charged cylinder in solution. *Biopolymers.* 12:559–574.

Bella, J., B. Brodsky, and H. Berman. 1995. Hydration structure of a collagen peptide. *Structure.* 3:893–906.

Bella, J., M. Eaton, B. Brodsky, and H. M. Berman. 1994. Crystal and molecular structure of a collagen-like peptide at 1.9 Å resolution. *Science.* 266:75–81.

Bloomfield, V. A. 1996. DNA condensation. *Curr. Opinion Struct. Biol.* 6:334–341.

Crothers, D. M., J. Drak, J. D. Kahn, and S. D. Levene. 1992. DNA bending, flexibility and helical repeat by cyclization kinetics. *In* Methods in Enzymology. D. M. J. Lilley and J. E. Dahlberg, editors. Academic Press, San Diego. 3–29.

Edwards, K. J., D. G. Brown, N. Spink, and S. Neidle. 1992. Molecular structure of the B-DNA dodecamer d(CGCAAATTTGCG)2. An examination of propeller twist and minor-groove water structure at 2.2 Å resolution. *J. Mol. Biol.* 226:1161–1173.

Fraser, R. D. B. and T. P. MacRae. 1973. Conformation in Fibrous Proteins. Academic Press, New York.

Gosule, L. C. and J. A. Schellman. 1978. DNA condensation with polyamines. I. spectroscopic studies. *J. Mol. Biol.* 121:311–326.

Israelachvili, J. and H. Wennerstrom. 1996. Role of hydration and water structure in biological and colloidal interactions. *Nature.* 379:219–225.

Jayaram, B. and D. L. Beveridge. 1990. Free energy of an arbitrary charge distribution imbedded in coaxial cylindrical dielectric continua: application to conformational preferences of DNA in aqueous solutions. *J. Phys. Chem.* 94:4666–4671.

Jayaram, B., K. A. Sharp, and B. Honig. 1989. The electrostatic potential of B-DNA. *Biopolymers.* 28:975–993.

Knoll, D. A., M. D. Fried, and V. A. Bloomfield. 1988. Heat-induced DNA aggregation in the presence of divalent metal salts. *In* DNA and its Drug Complexes. R. H. Sarma and M. H. Sarma, editors. Adenin Press, New York. 123–145.

Kornyshev, A. A. and S. Leikin. 1989. Fluctuation theory of hydration forces: The dramatic effects of inhomogeneous boundary conditions. *Phys. Rev. A.* 40:6431–6437.

Kornyshev, A. A. and S. Leikin. 1997. Theory of interaction between helical molecules. *J. Chem. Phys.* 107:3656–3674; Erratum 108:7035.

Kornyshev, A. A., and S. Leikin. 1998. Electrostatic interaction between helical macromolecules in dense aggregates. An impetus for DNA poly- and meso-morphism. *Proc. Natl. Acad. Sci. USA.* (in press).

Kuznetsova, N., D. C. Rau, V. A. Parsegian, and S. Leikin. 1997. Solvent hydrogen-bond network in protein self-assembly: Solvation of collagen triple helices in non-aqueous solvents. *Biophys. J.* 72:353–362.

Leikin, S., V. A. Parsegian, D. C. Rau, and R. P. Rand. 1993. Hydration forces. *Annu. Rev. Phys. Chem.* 44:369–95.

Leikin, S., V. A. Parsegian, W. H. Yang, and G. E. Walrafen. 1997. Raman spectral evidence for hydration forces between collagen triple helices. *Proc. Natl. Acad. Sci. USA.* 94:11312–11317.

Leikin, S., D. C. Rau, and V. A. Parsegian. 1994. Direct measurement of forces between self-assembled proteins: temperature-dependent exponential forces between collagen triple helices. *Proc. Natl. Acad. Sci. USA.* 91:276–280.

Leikin, S., D. C. Rau, and V. A. Parsegian. 1995. Temperature-favoured assembly of collagen is driven by hydrophilic not hydrophobic interactions. *Nature Struct. Biol.* 2:205–10.

Mariani, P., F. Ciuchi, and L. Saturni. 1998. Helix-specific interactions induce condensation of guanosine four-stranded helices in concentrated salt solutions. *Biophys. J.* 74:430–435.

Mariani, P. and L. Saturni. 1996. Measurement of intercolumnar forces between parallel guanosine four-stranded helices. *Biophys. J.* 70: 2867–2874.

McIntosh, T. J. and S. A. Simon. 1994. Hydration and steric pressures between phospholipid bilayers. *Annu. Rev. Biophys. Biomol. Struct.* 23:27–51.

Parsegian, V. A. and E. A. Evans. 1996. Long and short range intermolecular and intercolloidal forces. *Curr. Opin. Colloid Interface Sci.* 1:53–60.

Pelta, J., F. Livolant, and J.-L. Sikorav. 1996. DNA aggregation induced by polyamines and cobalthexamine. *J. Biol. Chem.* 271:5656–5662.

Rau, D. C., B. Lee, and V. A. Parsegian. 1984. Measurement of the repulsive force between polyelectrolyte molecules in ionic solution: hydration forces between parallel DNA double helices. *Proc. Natl. Acad. Sci. USA.* 81:2621–2625.

Rau, D. C. and V. A. Parsegian. 1990. Direct measurement of forces between linear polysaccharides xanthan and schizophyllan. *Science.* 249:1278–1281.

Rau, D. C. and V. A. Parsegian. 1992a. Direct measurement of temperature-dependent solvation forces between DNA double helices. *Biophys. J.* 61:260–271.

Rau, D. C. and V. A. Parsegian. 1992b. Direct measurement of the intermolecular forces between counterion-condensed DNA double helices. Evidence for long range attractive hydration forces. *Biophys. J.* 61: 246–259.

Rhodes, D. and A. Klug. 1980. Helical periodicity of DNA determined by enzyme digestion. *Nature.* 286:573–578.

Saenger, W. 1984. Principles of Nucleic Acid Structure. Springer-Verlag, New York.

Soumpasis, D. 1978. Debye-Huckel theory of model polyelectrolytes. *J. Chem. Phys.* 69:3190–3196.

Wagner, K., E. Keyes, T. W. Kephart, and G. Edwards. 1997. Analytical Debye-Huckel model for electrostatic potentials around dissolved DNA. *Biophys. J.* 73:21–30.

Watson, J. D. and F. H. C. Crick. 1953. Molecular structure of nucleic acids. *Nature.* 171:737–738.

Widom, J. and R. L. Baldwin. 1983. Monomolecular condensation of λ-DNA induced by cobalt hexamine. *Biopolymers.* 22:1595–1620.

Wilkins, M. H. F., A. R. Stokes, and H. R. Wilson. 1953. Molecular structure of deoxypentose nucleic acids. *Nature.* 171:738–740.

Zimmerman, S. B. and B. H. Pheiffer. 1979. Helical parameters of DNA do not change when DNA fibers are wetted: X-ray diffraction study. *Proc. Natl. Acad. Sci. USA.* 76:2703–2707.